Symmetry based analysis of the Kohn anomaly and electron-phonon interaction in graphene and carbon nanotubes

I. Milošević,[1,*] N. Kepčija,[1] E. Dobardžić,[1] M. Mohr,[2] J. Maultzsch,[2] C. Thomsen,[2] and M. Damnjanović[1]
[1]*NanoLab, Faculty of Physics, University of Belgrade, Studentski Trg 12, 11001 Belgrade, Serbia*
[2]*Institut für Festkörperphysik, Technische Universität Berlin, Hardenbergstrasse 36, 10623 Berlin, Germany*
(Received 20 March 2010; revised manuscript received 3 June 2010; published 30 June 2010)

Symmetry based analysis of the electron-phonon coupling in graphene and carbon nanotubes is performed and Kohn anomalies, their Brillouin-zone positions together with the complete set of good quantum numbers are predicted. Interestingly, graphene dynamical representation is found to contain only a small portion of quite a large set of inequivalent irreducible representations of the relevant full symmetry group. Besides, vanishing of the electron-phonon interaction for majority of the normal displacements is also shown to be a consequence of the symmetry. The results are further numerically confirmed within full and tight-binding density-functional calculations and force constants model and enhanced coupling to the Fermi level electrons of the Dirac point A_{1g} mode with respect to the Γ point E_{2g} mode is confirmed. Finally, energy dispersion of the kink phonon spectrum is analytically evaluated and compared to the classical phonon spectrum.

DOI: 10.1103/PhysRevB.81.233410 PACS number(s): 81.05.ue, 88.30.rh, 31.15.xh, 63.22.Rc

Graphene[1,2] being an exciting and unusual material in many respects and having prospects of a new technological marvel attracts tremendous attention of quite a wide spectrum of researches. Kohn anomaly[3] pertains to the most important fundamental topics of graphene physics due to its relevance for Raman spectroscopy which has an essential role in investigating this, in many ways unique two-dimensional (2D) surface being thus easily accessible to Raman scattering measurements.[4] Namely, electron-phonon coupling is particularly interesting in graphitic materials due to their specific pointlike Fermi surface. In graphene it is electron-phonon coupling which strongly softens phonon frequencies giving rise to Kohn anomalies which occur for phonons having wave number q such that there are two electronic states k_1 and $k_2=k_1+q$ at the Fermi surface. In the phononic spectrum of a metal a Kohn anomaly is manifested as discontinuity in the derivative of the dispersion relation that occurs at certain points of the Brillouin zone (BZ), produced by the abrupt change in the screening of lattice vibrations by conduction electrons. In graphene, the electronic gap vanishes only at the two equivalent K Brillouin-zone points (the so called Dirac points because of the linear dispersion corresponding to the massless Dirac fermions) which are connected by the vector K. Thus, Kohn anomalies can occur for central, Γ point phonons and $q=K$, Dirac point phonons. Also, in metallic single-wall carbon nanotubes the Fermi surface consists of only two points and Kohn anomalies occur only for phonons with zero wave vector or with the wave vector q connecting these two Fermi-surface points. Due to their quasi-one-dimensionality the armchair carbon nanotubes are expected to exhibit stronger Kohn anomaly than graphene.[5,6]

In this Brief Report we use full symmetry of graphene[7] and carbon nanotubes[8] in order to discuss electron-phonon interaction and to point out the direct consequences of symmetry, completely independent on the model of dynamics used. The symmetry-based results are further numerically confirmed within full and tight-binding density-functional calculations and force constants model.

Graphene, one-atom-thick allotrope of carbon with a honeycomb structure made out of hexagons, is a two-dimensional crystal with diperiodic symmetry[9] group DG80 $=\mathbf{TD}_{6h}$ (the symmetry generators are shown in Fig. 1). For considerations restricted to the in-plane modes, horizontal mirror symmetry can be ignored and normal subgroup $\mathbf{C}_{6v}$ of the full symmetry group $\mathbf{D}_{6h}$ can be used[10]). Note that DG80 is not a subgroup of the nonsymmorphic space group $P6_3/mmc$ of graphite.[11] Graphene is a single orbit system, generated by the subgroup DG3$=\mathbf{TC}_2$, with the stabilizer isomorphic to $\mathbf{D}_{3h}$. Despite this large stabilizer with twelve elements, graphene is not invariant under any Euclidean supergroup. However, its dynamical representation D^{dyn} contains only a small portion of quite a large set of inequivalent irreducible representations of DG80. It is symmetry which also predicts vanishing of the electron-phonon interaction for many normal displacements.

Decomposition of the dynamical representation onto the irreducible components[7] is

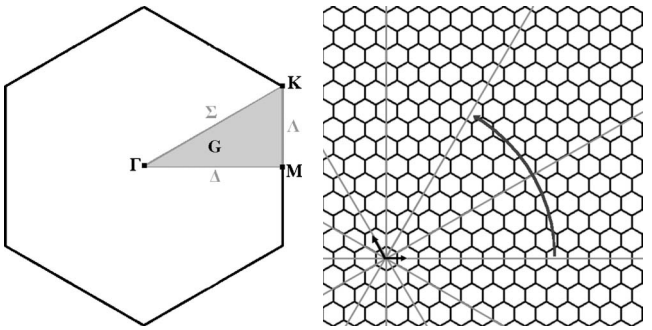

FIG. 1. Right panel: Brillouin zone and irreducible domain of graphene. Notation of the high symmetry lines and points, as well as of the interior domain, are introduced. Left panel: graphene symmetry generators: 2D translations, rotation for $\pi/3$, horizontal and vertical mirror reflections.

$$D^{\mathrm{dyn}} = \sum_{\mathbf{k}} (2^0_{\mathbf{k}}G^-_0 + 4^0_{\mathbf{k}}G^+_0) + 2\sum_k ({}^{-1}_k\Delta^+_0 + {}^1_k\Delta^-_0 + {}^1_k\Delta^+_0)$$
$$+ \sum_k ({}^{-1}_k\Lambda^-_0 + 2\,{}^{-1}_k\Lambda^+_0 + {}^1_k\Lambda^-_0 + 2\,{}^1_k\Lambda^+_0)$$
$$+ \sum_k ({}^{-1}_k\Sigma^-_0 + 2\,{}^{-1}_k\Sigma^+_0 + {}^1_k\Sigma^-_0 + 2\,{}^1_k\Sigma^+_0) + {}^1\Gamma^-_0 + {}^{-1}\Gamma^-_3$$
$$+ {}^0\Gamma^+_1 + {}^0\Gamma^+_2 + {}^{-1}M^+_0 + {}^1M^-_0 + {}^1M^+_0 + {}^{-1}M^-_1 + {}^{-1}M^+_1$$
$$+ {}^1M^+_1 + {}^1K^+_0 + {}^0K^+_0 + {}^0K^-_1 + {}^0K^+_1, \quad (1)$$

where the labels of the components ${}^v_kX^h_m$ follow notation of the irreducible domain (ID) of graphene shown in Fig. 1 and indicate the full set of conserved quantum numbers: **k** is wave vector, v and h are vertical and horizontal mirror parities, taking values ± 1 (even/odd) and 0 (not defined), while m is angular quantum number. Dimensions of the irreducible representations are as follows: 12-dimensional G from the interior of the graphene ID; six-dimensional Δ, Λ and Σ (special lines of the ID), four-dimensional K_1 (high symmetry point K), three-dimensional M (high symmetry point M), two-dimensional K_0, Γ_1, and Γ_2 (high symmetry points K and Γ), and one-dimensional Γ_0 and Γ_3.

The electronic states transform according to the following representation:

$$D^{\mathrm{el}}(G) = 2\sum_{\mathbf{k}} {}^0_{\mathbf{k}}G^-_0 + 2\sum_k {}^1_k\Delta^-_0 + \sum_k ({}^{-1}_k\Lambda^-_0 + {}^1_k\Lambda^-_0)$$
$$+ \sum_k ({}^{-1}_k\Sigma^-_0 + {}^1_k\Sigma^-_0) + {}^0K^-_1 + {}^1M^-_0 + {}^{-1}M^-_1 + {}^1\Gamma^-_0$$
$$+ {}^{-1}\Gamma^-_3, \quad (2)$$

where k takes values from the interior of the ID of the Brillouin zone. It is primary the symmetry which substantially reduces the electron-phonon coupling. Namely, an electronic state transforming according to an irreducible representation $D^{(\mu)}$ can couple only to phonons transforming according to the irreducible representations contained in symmetrized square of $D^{(\mu)}$. Note that this condition when applied to the Fermi point states directly selects the Kohn modes. It turns out that only three, (out of six) optical modes at the Brillouin-zone center Γ and at Dirac point K are symmetry allowed to couple to Fermi electrons, i.e., only three optical phonons: ${}^0\Gamma^+_2$, ${}^1K^+_0$, and ${}^0K^+_1$ (E_{2g}, A_{1g}, and E^+_1 in the point group notation) can cause the Kohn anomaly. Remarkably, the remaining three phonons ${}^{-1}\Gamma^-_3$, ${}^{-1}K^+_0$, and ${}^0K^-_0$ (i.e., B_{3g}, E^{B}_0, and E^-_1) do not couple not only to Fermi but to any electrons.

The full picture of the electron-phonon interaction is schematically presented in Fig. 2 where electronic states and normal modes of vibration are listed according to their quantum numbers. The bold lines connect coupled electronic states and normal modes. The dashed lines indicate that the coupling between the two sets of the electrons and phonons is only for some values of the wave vector. For instance, the uppermost dashed line on the left side of Fig. 2 is meant to show that some (but not all) normal modes having wave vector which belongs to Δ line, zero angular momentum, even vertical and odd horizontal mirror parity are coupled to some (but not to all) electrons having wave vector from ID interior, zero angular momentum and odd horizontal mirror parity.

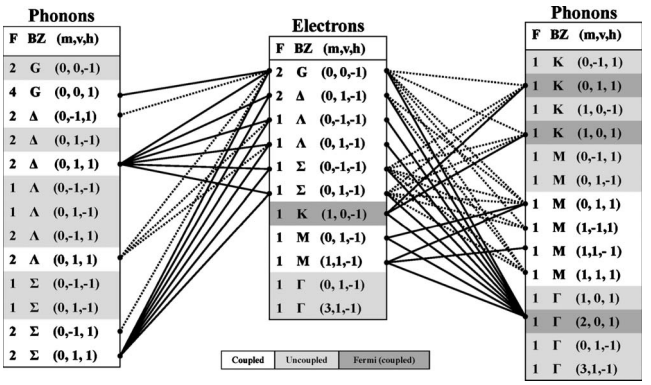

FIG. 2. Electron-phonon interaction in graphene. Electrons and phonons are assigned by the complete set of quantum numbers: **k** (takes the values allowed by the position BZ within Brillouin zone) and (m,v,h) give ${}^v_{\mathbf{k}}X^h_m$. F is frequency number. Coupled states and modes are connected by bold lines; the dashed lines indicate coupling for only some k values (not all allowed by BZ).

Quite evidently, the vast majority of the graphene normal modes are not coupled to any electrons: all Λ phonons, zero angular momentum phonons from the interior of ID with odd horizontal mirror parity, also zero angular momenta phonons with even horizontal mirror parity and wave vector lying on the special line Σ, likewise the acoustic Γ point phonons E^+_1 and A^-_0 and optical phonons ${}^{-1}M^+_0$, ${}^1M^-_0$, and ${}^{-1}M^-_1$, together with the already mentioned optical, but not Kohn, Γ- and K-point phonons B_{3g}, E^{B}_0, and E^-_1. Such a number of the vibronically uncoupled nonsymmetric modes contribute to the stability of the honeycomb lattice.

Phonon dispersions have been calculated within symmetry based force constants approach;[12] however, as frequency of the irreducible representations of the Γ-point and K-point modes in the dynamical representation, (1), is one, the geometry of their displacements is fully determined by the symmetry, thus being totally independent of the dynamical model (unlike the corresponding frequencies). Further, for these modes the electronic band structure is calculated as a function of elongation by *ab initio* and tight-binding density-functional (DFTB) method.[13] This enables to derive dependence of the electronic total energy and the band gap on the elongation. It is remarkable that total energy in the *ab initio* approach (which includes only translational periodicity of the system) has usual parabolic behavior while full symmetry based DFTB approach leads to the potential which is nicely approximated by the kinklike intersection of two parabolas (M, ω, and a are their parameters)

$$V(x) = \frac{1}{2}M\omega^2(x \pm a)^2 \quad (3)$$

(bolded curve in Fig. 3, upper panel). Note that disagreements stemming from these two methods are hardly verifiable experimentally. Namely, the spectrum corresponding to the potential V is

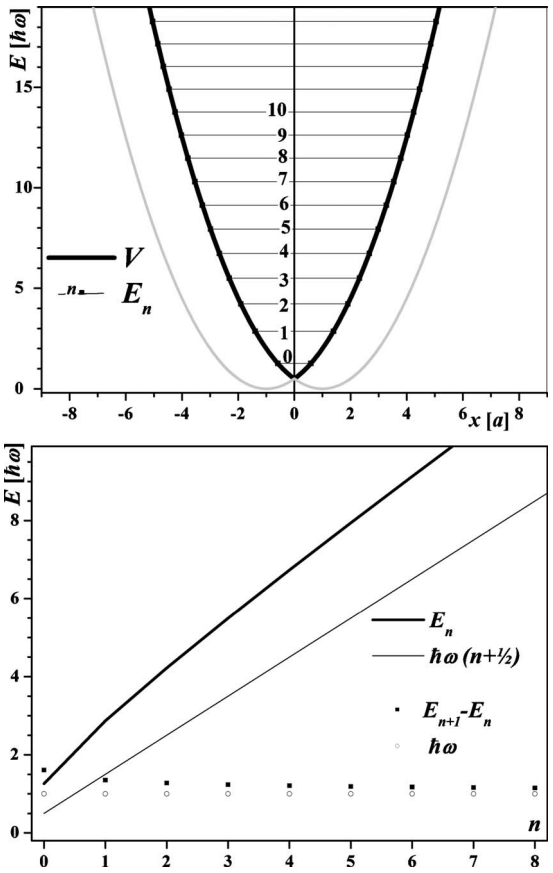

FIG. 3. Spectrum of the kink phonons. Upper panel: potential approximated by intersection of two harmonic potentials and ground energy, and overtones of kink phonons. Lower panel: kink phonon (black) energy function E_n, Eq. (4), and differences between adjacent kink-phonon energy levels in comparison to the ordinary phonons (gray).

$$E_n = \hbar\omega\left[f(n) + \frac{1}{2}\right], \quad (n = 0,1,2,\ldots),$$

$$f(n) = n + a\sqrt{\frac{M\omega}{\hbar}}\sqrt{0.13 + 0.81n} + 0.4a\sqrt{\frac{M\omega}{\hbar}}. \quad (4)$$

As shown in Fig. 3, lower panel, it is almost equidistant, and the deviations of "kink phonons" from the usual (parabolic) ones are measurable for the lowest energy states only.

Assigned by the complete set of quantum numbers, the electronic bands are given in Fig. 4. The phonon dispersions exhibit two kinks, for phonons $\Gamma(2,0,1)$ and $K(0,1,1)$ which are symmetry allowed to couple to the Fermi electrons. These normal displacements are illustrated in Fig. 5. Their frequencies are 1577 cm^{-1} and 1294 cm^{-1}, respectively.

The electron-phonon coupling has been further analyzed within the electron-phonon deformation potential approximation.[14] Namely, the electron-phonon matrix element $\mathcal{M}_{\text{el-ph}}$ is well approximated by the following formula:

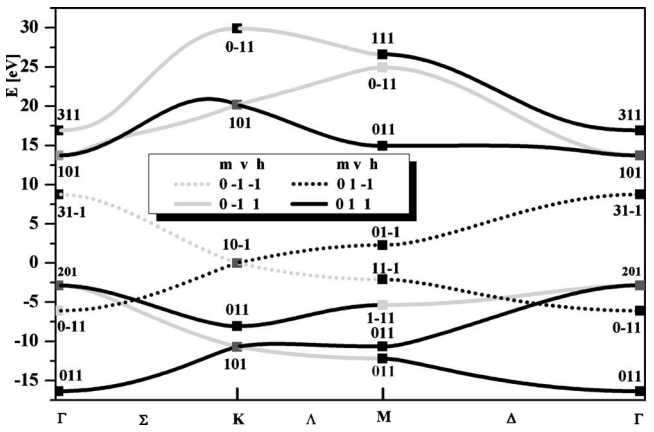

FIG. 4. Graphene electronic band structure along the symmetry directions assigned by the complete set of quantum numbers.

$$\mathcal{M}_{\text{el-ph}} = \langle\Psi_e|\frac{dV(u)}{du}|\Psi_e\rangle, \quad (5)$$

where Ψ_e is the electronic wave function, $V(u)$ is the effective one-electron potential, and u is the phonon elongation.

We calculate Fermi-level dependence on the all six Γ and K optical phonons displacements as a function of elongation. As can be seen from Fig. 6 only the Kohn modes have substantial impact on the Fermi level, opening a finite gap. Also, the numerical simulations show that the substantial change in the electronic energy stems only from the coupling to the two Kohn phonons and that it is more pronounced for the Dirac point Kohn mode.

Symmetry of the armchair nanotube (n,n) is described by the line group[8] $\mathbf{L}2n_n/mcm = \mathbf{T}^1_{2n}\mathbf{D}_{n\text{h}}$. The Fermi point k_F is at the crossing of the bands ${}_kE^1_n$ and ${}_kE^{-1}_n$ (corresponding states have angular quantum number $m=n$), which is close to $2\pi/3a$. Symmetrized square of the Fermi state irreducible representations decompose onto the totally symmetric representation ${}_0A^+_0$ and double degenerate representation ${}_{2k_F}E^1_n$ (of course, instead of $2k_F$ its equivalent point from the Brillouin zone is taken). These representations pertain to the dynamical representation of the tube with the frequency numbers $f_A=2$ (radial breathing and high-energy mode, denoted by RB and HE) and $f_E=3$ (since E is double degenerate, this gives three pairs of modes denoted by E_1, E_2, and E_3), re-

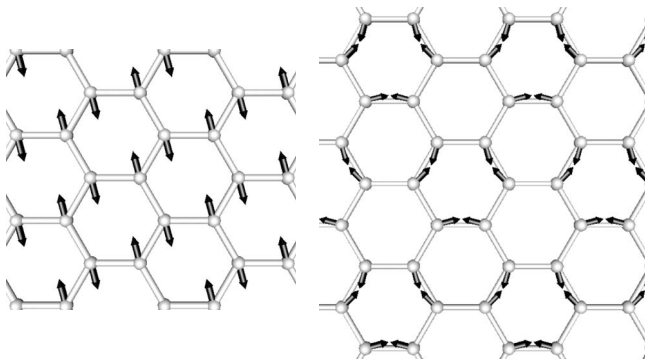

FIG. 5. Kohn normal mode displacements E_{2g} and A_{1g}.

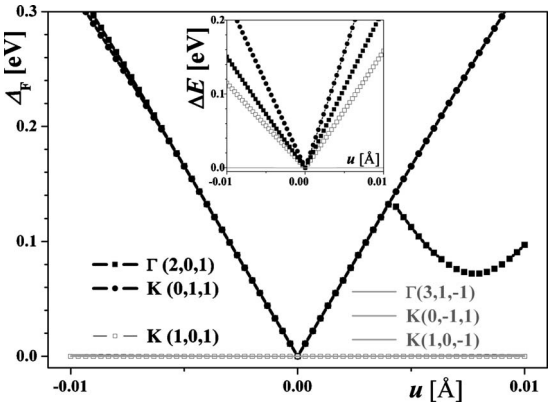

FIG. 6. Gap and total energy (inset) as functions of the elongation of the optical phonons at Γ and *K*. Evidently, the substantial gap opening comes from the Kohn modes displacements only.

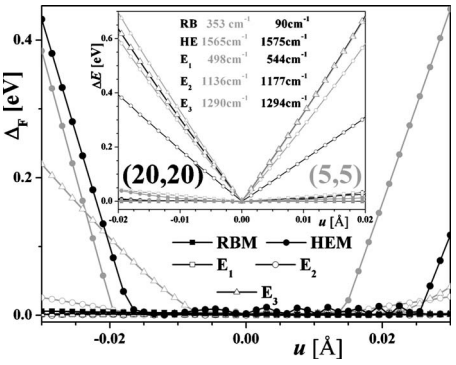

FIG. 7. Gap and total energy (inset) as functions of the elongation of the optical phonons at Γ and $2k_F$ of (5,5) (with $k_F=41\pi/67a$) and (20,20) ($k_F=50\pi/73a$) nanotubes.

spectively. As shown in inset of Fig. 7, total coupling to electrons is much stronger for *E* modes. However, the strongest coupling to the Fermi level is for the high-energy mode, causing substantial electronic band-gap opening; also, in accordance with the previous predictions,[6,15] for the (5,5) tube E_3 mode shows the same effect.

In summary, symmetry predicts the Brillouin-zone position of the Kohn phonons and their spatial displacements, assigning them by the full set of conserved quantum numbers. Apart form the acoustic phonons most of the K- and Γ-point optical phonons are not coupled to any electrons, which is shown to be the characteristic of graphene structure. All these findings are completely model independent.

Numerical symmetry based analysis of the electron-phonon coupling shows that Kohn anomaly in armchair carbon nanotubes is stronger than in graphene and more pronounced in narrow nanotubes. Deformation potential matrix element estimations show the influence of the Kohn modes vibrations on the Fermi energy oscillations, causing thus the electronic band-gap opening. If tunable, these band-gap oscillations could open a room for electronic applications.

In epitaxial graphene Kohn anomaly has been identified as the main scattering channel responsible for the high-resolution angle-resolved photoemission spectroscopy kink.[16] Here calculated frequencies of the Kohn modes agree very well with these spectroscopy measurements. Also, the enhanced coupling to the Fermi level electrons of the totally symmetric Dirac point Kohn mode with respect to the double degenerate Γ-point Kohn mode is confirmed.

Finally, energy dispersion of the kink-phonon spectrum is analytically evaluated and found to be similar to the classical phonon spectrum.

This work is supported by Serbian Ministry of Science (Project No. ON141017).

*ivag@rcub.bg.ac.rs; http://www.nanolab.rs

[1] K. S. Novoselov, A. K. Geim, S. V. Morozov, D. Jiang, Y. Zhang, S. V. Dubonos, I. V. Gregorieva, and A. A. Firsov, Science **306**, 666 (2004).
[2] A. K. Geim, Science **324**, 1530 (2009).
[3] W. Kohn, Phys. Rev. Lett. **2**, 393 (1959).
[4] M. S. Dresselhaus, A. Jorio, M. Hofmann, G. Dresselhaus, and R. Saito, Nano Lett. **10**, 751 (2010).
[5] S. Piscanec, M. Lazzeri, F. Mauri, A. C. Ferrari, and J. Robertson, Phys. Rev. Lett. **93**, 185503 (2004).
[6] S. Piscanec, M. Lazzeri, J. Robertson, A. C. Ferrari, and F. Mauri, Phys. Rev. B **75**, 035427 (2007).
[7] I. Milošević, B. Nikolić, M. Damnjanović, and M. Krčmar, J. Phys. A **31**, 3625 (1998).
[8] M. Damnjanović and I. Milošević, *Line Groups in Physics* (Springer-Verlag, Berlin, 2010).
[9] *International Tables for Crystallography, Volume E: Subperiodic Groups*, edited by V. Kopsky and D. B. Litvin (Kluwer, Dordrecht, 2002).
[10] J. L. Mañes, Phys. Rev. B **76**, 045430 (2007).
[11] L. M. Malard, M. H. D. Guimarães, D. L. Mafra, M. S. C. Mazzoni, and A. Jorio, Phys. Rev. B **79**, 125426 (2009).
[12] M. Mohr, J. Maultzsch, E. Dobardžić, S. Reich, I. Milošević, M. Damnjanović, A. Bosak, M. Krisch, and C. Thomsen, Phys. Rev. B **76**, 035439 (2007).
[13] I. Milošević, B. Nikolić, E. Dobardžić, M. Damnjanović, I. Popov, and G. Seifert, Phys. Rev. B **76**, 233414 (2007).
[14] F. S. Khan and P. B. Allen, Phys. Rev. B **29**, 3341 (1984).
[15] R. Barnett, E. Demler, and E. Kaxiras, Phys. Rev. B **71**, 035429 (2005).
[16] S. Y. Zhou, D. A. Siegel, A. V. Fedorov, and A. Lanzara, Phys. Rev. B **78**, 193404 (2008).